water

MDPI

Article

Real-Time Pyrolysis Dynamics of Thermally Aged Tire Microplastics by TGA-FTIR-GC/MS

Guangteng Bai [1,2,3], Juyang Fu [2], Qian Zhou [2,*] and Xiangliang Pan [1,2,*]

[1] Xinjiang Key Laboratory of Environmental Pollution and Bioremediation, Xinjiang Institute of Ecology and Geography Chinese Academy of Sciences, Urumqi 830011, China
[2] Key Laboratory of Microbial Technology for Industrial Pollution Control of Zhejiang Province, College of Environment, Zhejiang University of Technology, Hangzhou 310014, China
[3] University of Chinese Academy of Sciences, Beijing 100049, China
* Correspondence: qianzhou@zjut.edu.cn (Q.Z.); panxl@zjut.edu.cn (X.P.)

Abstract: Tire wear particles (TWPs), as a type of thermosetting microplastic (MP), accumulate in aquatic environments due to their wide application in road traffic globally. The increase in temperature because of friction heat may cause aging of tire materials, inducing water evaporation, additive volatilization, polymer decomposition, and may pose serious potential risks to aquatic and terrestrial ecosystems. However, research on real-time pyrolysis dynamics of thermally aged tire MPs is very limited. In this study, a thermogravimetric analyzer coupled with Fourier transform infrared spectrometry and gas chromatography-mass spectrometry (TG-FTIR-GC/MS) was used to investigate pyrolysis behaviors and products of thermally aged tire MPs. FTIR analysis indicated that the main pyrolysis gases included carbon dioxide, carbon monoxide, aliphatic compounds, aromatic compounds and carbonyl compounds. The GC/MS analysis further determined the main pyrolytic products, including methylbenzene, styrene, m-xylene and D-limonene. These data combined with TG analysis revealed that the main pyrolytic products of TWPs were released at 400–600 °C. Moreover, the results showed that the number of aliphatic/aromatic compounds released increased in short-term thermo-oxidative aging but decreased in long-term thermo-oxidative aging. Moreover, the aged TWPs presented higher released amounts of styrene and methylbenzene but lower amounts of D-limonene compared to the original TWPs. These results can provide new insights into the evaluation method of TWP aging and a better understanding on TWP fate in aquatic and terrestrial environments.

Keywords: tire microplastics; thermal aging; volatile products; TG-FTIR-GC/MS

Citation: Bai, G.; Fu, J.; Zhou, Q.; Pan, X. Real-Time Pyrolysis Dynamics of Thermally Aged Tire Microplastics by TGA-FTIR-GC/MS. *Water* **2023**, *15*, 1944. https://doi.org/10.3390/w15101944

Academic Editor: Grzegorz Nałęcz-Jawecki

Received: 7 April 2023
Revised: 15 May 2023
Accepted: 17 May 2023
Published: 21 May 2023

1. Introduction

Tires have wide applications in road traffic globally due to their advantages of high elasticity and cost-effectiveness [1]. It was estimated that roughly 19 million tons of tires were produced in 2019 and the global production grows every year by several million tons [2]. However, tires suffer wear as a result of the contact between the road surface and a tire in motion, leading to emissions of tire wear particles (TWPs) [3,4]. In addition, a large number of waste tires are discarded into the environment each year worldwide because of mismanagement, which might form TWPs due to the aging process [5]. TWPs are considered thermosetting microplastics (MPs) since they contain synthetic rubber, and tire abrasion is demonstrated to be the greatest source of MPs from road traffic [6]. There is an estimation that roughly 6 million tons of TWPs enter the environment every year due to the global development of automobile traffic [7]. These TWPs are not easily degraded due to a variety of stabilizers and the cross-linked structure created by the vulcanization process in tire manufacturing, leading to a huge accumulation in various environments including soil, water and atmosphere through wind, road runoff and passing vehicles [1]. Recently, environmental TWPs have been determined with concentrations of 0.6–5.0 mg L^{-1} in

river water and 400.0–2200.0 μg g^{-1} in river sediments, and their size ranges from a few nanometers to several hundred micrometers [8,9].

Moreover, the contact between a tire in motion and the road surface will produce friction heat with a relatively high temperature of up to 100–200 °C [10]. The increase in temperature may cause aging of the tire material (including TWPs), which might further lead volatile tire components to evaporate [1]. Previous studies have demonstrated that elevated temperature increases oxygen diffusion in tire materials, promoting chain scission and additional crosslinking due to oxidation reactions, leading to a decrease in the viscosity and an increase in the rigidity of the material [11,12]. Consequently, molecular weight might be reduced and cracks may form on the surface of the tire material [13]. Furthermore, thermomechanical processes can generate ultrafine particles (<0.1 μm) from tire surfaces via rapid condensing of volatile tire constituents vaporized by high temperature [14,15]. However, the thermal aging process and its characterization on TWPs have been very limited until now. A recent study reported that small cracks and holes were produced on TWP surfaces and the specific surface areas increased after aging, which enhanced the carrier effects of TWPs on environmental pollutants such as antibiotics [16]. Moreover, the aging of TWPs might cause changes in particle composition and release of additives, such as antioxidants, crosslinking agents, and processing aids [17–19], which may pose serious potential risks to the environmental ecosystem [20,21]. Therefore, research on thermal aging processes of TWPs is important to assess the environmental fate and potential risk of the TWPs in aquatic and terrestrial ecosystems.

Flourier transform infrared spectroscopy (FTIR), pyrolysis gas chromatography/mass spectrometry (Py-GC/MS) and thermogravimetric analysis-based GC/MS (TGA-GC/MS) are widely used for the analysis of chemical functional groups and pyrogenic products formed from aging polymeric materials [22,23]. In recent years, FTIR analysis has been applied to analyze surface alterations of rubber exposed to an elevated temperature of 70 °C. However, FTIR can lead to poor-quality spectra resulting from colored particles when using transmission mode, and it is unable to provide detailed information on components of aging TWPs [24]. Py-GC/MS is an effective approach to quantitatively analyze thermal decomposition products of aging TWPs, but it only provides compound structures at certain pyrolysis temperatures and it cannot obtain specific bonds of aging TWPs [25,26]. In order to combine the advantages of the both, a thermogravimetric analyzer coupled with Fourier transform infrared spectrometry and gas chromatography-mass spectrometry (TG-FTIR-GC/MS) was introduced in the application of plastic polymer materials [27,28]. This approach incorporates the aforementioned techniques into a single instrument, which can simultaneously collect physical (such as thermal properties) and chemical information on plastic particles to maximize the possibility of identifying the pyrolytic component [29]. Therefore, the efficiency, real-time process, and simplification make it a potential approach for aging TWP analysis as compared to the conventional waste tire analytical technology.

In the present study, TWPs were prepared via abrasion tests of rubber tire materials for heating and aging at a high temperature, aiming to simulate the thermal aging process of TWPs caused by friction heat generated from emergency braking or contact between motor vehicles and roads. Thermodynamics, pyrolysis behaviors and gas products of aging TWPs were focally analyzed using TG-FTIR-GC/MS. The aims of the current study are: (1) to characterize the thermodynamics of thermally aged TWPs; (2) to identify chemical bonds and gas products of thermally aged TWPs; and (3) to compare the difference in dynamic pyrolysis behaviors of TWPs with thermal aging time. We anticipate that this will provide new insights into the evaluation method of TWP aging and a better understanding of the fate of TWPs in the environment.

2. Materials and Methods

2.1. Sample Preparation and Thermal Aging

The tire products were purchased from Youao Rubber Products Co., LTD (Xingtai, China). Firstly, the experimental tire materials were washed using pure water and air-dried

in a clean bench. Then, they were ground into small particles (below 100 µm) using an electric grinder and a mesh sieve with pore size of 100 µm. The samples with a size of below 100 µm were collected and placed into desiccators for subsequent experiments.

In general, the contact between a tire in motion and the road surface produces friction temperatures of 100–200 °C [10]. The authors hypothesized that the temperature between a tire in motion and the road surface caused by emergency braking or a vehicular fire accident would be higher, and could reach 400 °C. Therefore, the collected samples were placed on a clean stainless-steel plate and then the plate and samples were heated through an electric stove with a high temperature of 400 °C (Figure 1). The samples were then collected into pre-washed glass petri dishes after heat aging for 3 min (named stage I) and 6 min (named stage II), respectively. The samples with different heating time simulated different thermal-aging degrees of TWPs caused by real friction heat generation between tires and road surfaces. The photos and corresponding descriptions of morphologies of TWPs with different thermal aging times are shown in Figure S1 and Text S1.

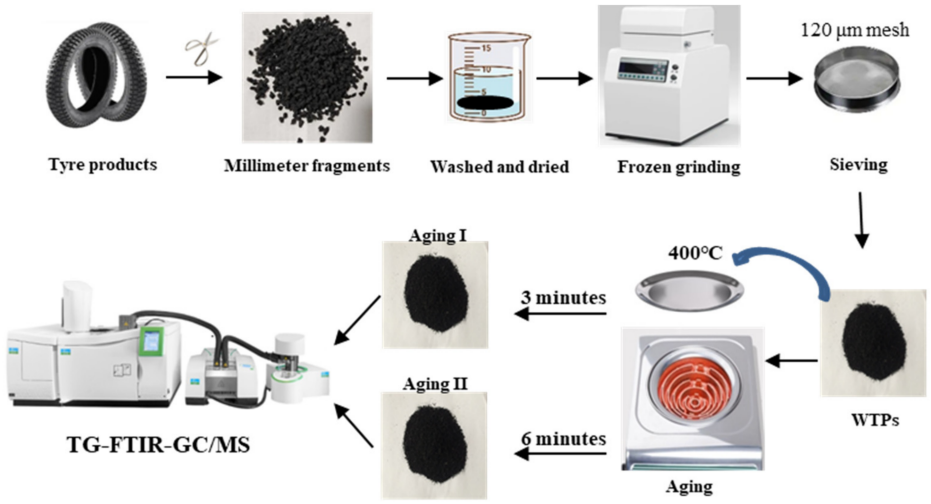

Figure 1. The schematic procedure of sample preparation, thermal aging and TG-GC-MS analysis.

2.2. TG-FTIR-MS Experiments

The TWPs with different aging times (aging I, aging II, and original state) were analyzed by an independent FTIR spectrometer (Frontier FTIR Spotlight 400, PerkinElmer, Shelton, WA, USA) to obtain preliminary infrared spectra before TG-FTIR-MS analysis (Figure S2). The resolution was 4 cm^{-1} with 32 scans in a scanning range from 4000 to 750 cm^{-1}. Then, a TG analyzer (Thermogravimetric Analyzer 4000, PerkinElmer, Shelton, WA, USA), a FTIR spectrometer and a MS instrument (Mass Spectrometer Clarus SQ8T, PerkinElmer, Shelton, WA, USA) were combined to detect the functional groups of the pyrolytic gases. In the TG experiments, 20.0 mg TWP samples were placed in Al_2O_3 crucibles and the temperature was held at 30 °C for 1 min. Then, the samples were heated from 30 to 900 °C with a heating rate of 10 °C/min at a 50 mL/min flow rate of the carrier gas (He) [30]. The resolution was 8 cm^{-1} with 4 scans in a scanning range from 4000 to 500 cm^{-1}. The evolved gas passed from FTIR cells through another transfer tube into an MS instrument. The MS was run with an EI source ionization energy of 70 eV and mass spectral data were obtained from 2–400 m/z. The temperature of the transfer tubes in the TG, FTIR and MS analyzers was kept at 260 °C to avoid experimental errors caused by gas condensation. In order to increase sample throughput, the total length of the GC-MS was set to coincide with the end of the TGA analysis.

2.3. TG-GC-MS Experiments

The gas products were focused on for further detection of the temperature point at which the sample had the highest weight loss rate. Firstly, the 20.0 mg same TWP

samples were placed in the TG analyzer and heated from 30 to 900 °C with a heating rate of 20 °C/min (other conditions were consistent with Section 2.2). Then, the gas produced at 470 °C with a peak at the highest weight loss rate was passed through a transfer tube into GC/MS. A GC instrument (Clarus 690, PerkinElmer, Shelton, WA, USA) was equipped with an Elite-5HT column at 40 °C, then the temperature increased at 10 °C/min until 260 °C and was kept at 260 °C for 10 min. The MS was run with an EI source ionization energy of 70 eV and mass spectral data were obtained from 2–400 m/z. All obtained mass spectra were matched and compared with standard spectra in the NIST MS Search library V2.2 to identify evolved gas products.

2.4. Data Process and Analysis

PyrisManager software (PerkinElmer, Shelton, WA, USA) was used to analyze the data collected by thermogravimetry. The DTG (derivative thermogravimetry) curve was divided into different peaks by the Gauss method. Three-dimensional (3D) infrared spectral data were analyzed using Spectrum TimeBase version 3.1.6 (PerkinElmer, Inc., UK); and mass spectrum data analysis was conducted using TurboMass Version 6.1.2 (PerkinElmer, Shelton, WA, USA). Infrared spectral peak fitting was processed using Peakfit software and relative figures were produced using Origin 2021.

3. Result and Discussion

3.1. Dynamic TG Characterization of TWPs with Aging Time

The (derivative) TG curves of the TWP under different aging conditions were exhibited in Figure 2. The original TWPs started to lose weight at 200 °C, whereas aged TWPs began to lose weight at 280 °C (Aging I) and 260 °C (Aging II), showing the temperature on initial degradation of TWP shifted to higher pyrolysis temperatures after thermal aging. This indicated that thermo-oxidative aging caused a lag time for gas release of TWPs. Prior research has demonstrated that the thermal degradation of waste rubber tires can be divided into three stages based on TG analysis. These include water evaporation and additive volatilization (stage one), natural rubber decomposition (stage two), and decomposition of synthetic rubber such as butadiene rubber and styrene butadiene rubber (stage three) [31]. In general, stage one usually occurs at temperatures below 310 °C in terms of tire rubber. Previous studies reported that the pyrolysis temperature of natural and synthetic rubbers ranged from 180–300 °C and 300–500 °C, respectively [32]. Therefore, a slight weight loss phenomenon for the TWPs at 0–300 °C might be due to the decomposition of natural rubbers [30]. Thermo-oxidative aging might induce an increase in the crosslinking density of rubber molecular chains, resulting in sample weight loss beginning at relatively higher temperatures compared to original samples [33,34].

TWPs under different thermo-oxidative aging conditions presented different peaks of weight loss in the DTG curve. In order to compare differences in peaks of weight loss between 200 and 600 °C, the DTG curve was divided into separated peaks using Gauss. As shown in Figure 2c, the original TWPs showed four obvious peaks of weight loss in the temperature ranges of 200–450 °C (fitting peak I), 336–476 °C (fitting peak II), 385–527 °C (fitting peak III), and 411–560 °C (fitting peak IV), separately. Accordingly, their peak temperatures corresponding to the maximum weight loss rate were 332 °C, 407 °C, 457 °C and 482 °C, respectively. Combined with the following IR-MS results and the previous literature, the fitting peaks I, II, III and IV were regarded as polyurethane, nature rubber, synthetic rubber and secondary pyrolysis products (such as isocyanate degradation product) [35]. However, the DTG curves of the thermo-oxidative aged TWPs only exhibited three peaks in the range of 200–600 °C, including peak I, peak II and peak IV (Figure 2d,e). Furthermore, the fitting peak area of aged TWPs decreased compared to original samples. This indicated that thermo-oxidative aging caused degradation of the components (polyurethane and rubber), influencing the pyrolysis reaction process of TWPs [19].

Moreover, the residue rates of TWPs in aging II were 50.53%, which is significantly higher than the original stage (32.83%) and aging I (32.83%). These results indicated that the residue rate of TWPs was not affected by short aging time (aging I) but increased when aging time increased (aging II). Similar studies have shown that the residue rate of plastics can increase after thermal oxidation, such as polypropylene and polyvinyl chloride, which is mainly due to the formation of high-temperature-resistant impurities in the process of thermal oxidation [19,36]. In the present study, a higher proportion of ash content in aged TWPs compared to original TWPs might be due to loss of evaporative components in aged TWPs during thermal aging process. The ash content is the important factor that affects the pyrolysis products. The high ash content can decrease the pyrolytic bio-oil yields but increase the residue contents [30]. In the current study, the higher residue rate of aged TWPs compared to the original ones suggested that the thermal oxygen aging process possibly produced more ash contents.

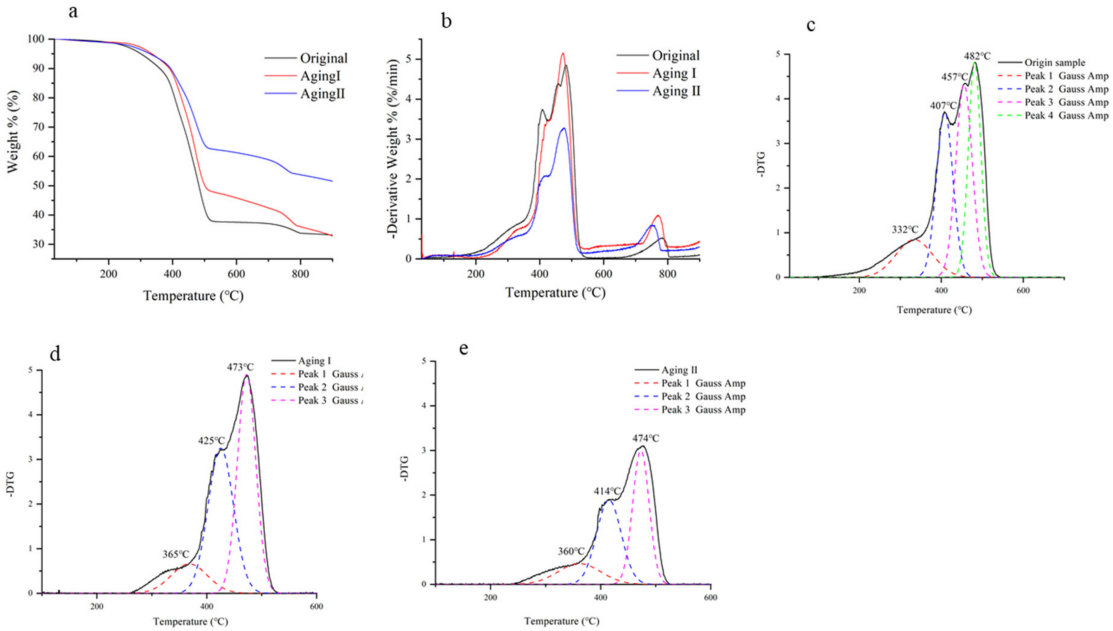

Figure 2. (Derivative) TG curves of TWPs pyrolysis under different aging conditions. (**a**), TG curves; (**b**), DTG curves; (**c**–**e**), division diagram on differential thermogravimetric peaks of TWPs under original stage, aging I and aging II.

3.2. Functional Groups of Pyrolytic Gases via TG-FTIR Analysis

3.2.1. TG-FTIR Characterization of Volatile Products

To investigate the evolution of volatiles release, the functional groups and gaseous products of tire pyrolysis process were detected in real time by using TG-FTIR. Different pyrolysis temperature stages were selected based on DTG curves for collecting FTIR spectra (Figure 3). The IR peaks, vibration and frequency ranges of the main functional groups can be seen in Table S1. The C-O-C stretching vibration in 1085 cm^{-1} at 220 °C (Figure 2b) indicated the emission of small molecule ether compounds due to decomposition of polyurethane in the initial stage [37]. The strong absorbance peaks in the range of 3100 cm^{-1}–2750 cm^{-1} and 1470 cm^{-1}–1300 cm^{-1} were attributed to the stretching vibration and bending vibration of C-H bonds of saturated aliphatic hydrocarbons, indicating that large quantities of alkanes were released. The peak of 3014 cm^{-1} might be attributed to CH_4, which can be formed from cleavage of -CH_3 and -CH_2- on the aliphatic hydrocarbon, as well as from the cracking of the alkyl chain of the aromatic ring.

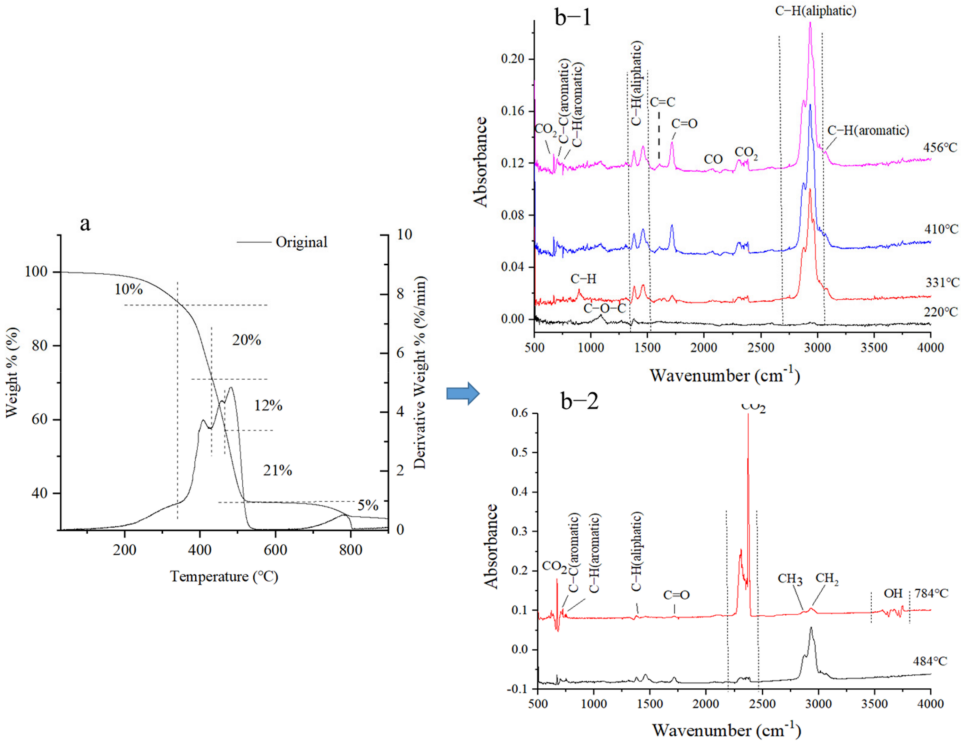

Figure 3. TG curves (**a**) and FTIR spectra (**b**) of original TWPs in inert atmosphere under different temperature. (**b-1**), FTIR spectra of original TWPs under 220−456°C; (**b-2**), FTIR spectra of original TWPs under 484−784 °C.

The absorbance peak belonging to CO_2 in 2350 and 668 cm^{-1} occurred throughout the pyrolysis temperature range, showing a gradual increase with the rise in pyrolysis temperature (Figure 2b,c). The CO_2 emission at the initial stage could be attributed to the decomposition of additives [38,39]. Subsequently, isocyanate was decomposed to release CO_2 with the increase in pyrolysis temperature, and CO_2 was produced by decomposition of inorganic matter sourced from the pyrolysis products of rubber material. The absorbance peaks at 750 and 700 cm^{-1} correspond to the out-of-plane bending vibrations of the C-H and C-C groups of aromatic benzene, respectively [40]. Furthermore, C=O stretching vibration in 1715 cm^{-1} and C=C vibration belonging to benzene ring in 1600 cm^{-1} were also observed during the pyrolysis process [37,41,42]. These main functional groups mean that the main pyrolysis products of TWPs contain hydrocarbons, aromatic compounds, carbonyl compounds, carbon dioxide and carbon monoxide.

In the present study, the types of functional groups of aged TWPs were more than those of the original TWPs, especially in the wave number range of 1900–1650 cm^{-1} and 3300–4000 cm^{-1} (Figure S1). For instance, a large quantity of peaks occurring in 1900–1650 cm^{-1} was attributed to C=O after thermal aging, indicating that TWPs experienced oxidation reactions under the thermal aging process [43,44]. In addition, the intensity of methylene CH_2 absorbance peaks at 2916 cm^{-1} and 2850 cm^{-1} and saturated alkyl absorption peaks at 1360~1470 cm^{-1} gradually decreased with the increase of high-temperature aging time. This indicated that methyl and methylene groups were destroyed and the main chains of rubber were degraded [45]. Previous studies have shown that the main chemical reactions of tire aging are crosslinking and decomposition [46]. In general, the main characteristic of the decomposition reaction is that the CH_2 group is oxidized and the C=C bond is not obviously damaged. On the contrary, the main characteristic of crosslinking reaction is that the C=C bond is cross-linked and the -CH_2 group has no obvious damage [47] (Zhang et al., 2020a). The results of the present study indicated that the oxidation decomposition was dominant during thermal aging at high temperatures.

3.2.2. Dynamic Change in Gas Products with Pyrolysis Temperature

The continuous dynamics of FTIR spectra on pyrolysis products with pyrolysis temperatures were analyzed to investigate the dynamic change in main gas products with pyrolysis temperatures and to compare their differences among TWPs under different aging conditions (Figure 4 and Figure S3). In general, the absorbance signal value at a specific wave number is linearly related to the gas concentration according to the Lambert–Beer law, and thus the change in absorbance signal value during the whole process can reflect the yield trend of gas components. In the current study, the evolution trends of various pyrolysis products were obtained by comparing the absorbance changes with temperature at specific wave numbers. Semi-quantitative comparison of pyrolysis products of TWPs under different aging conditions was conducted after absorbance of functional groups was normalized to equal sample weight [48].

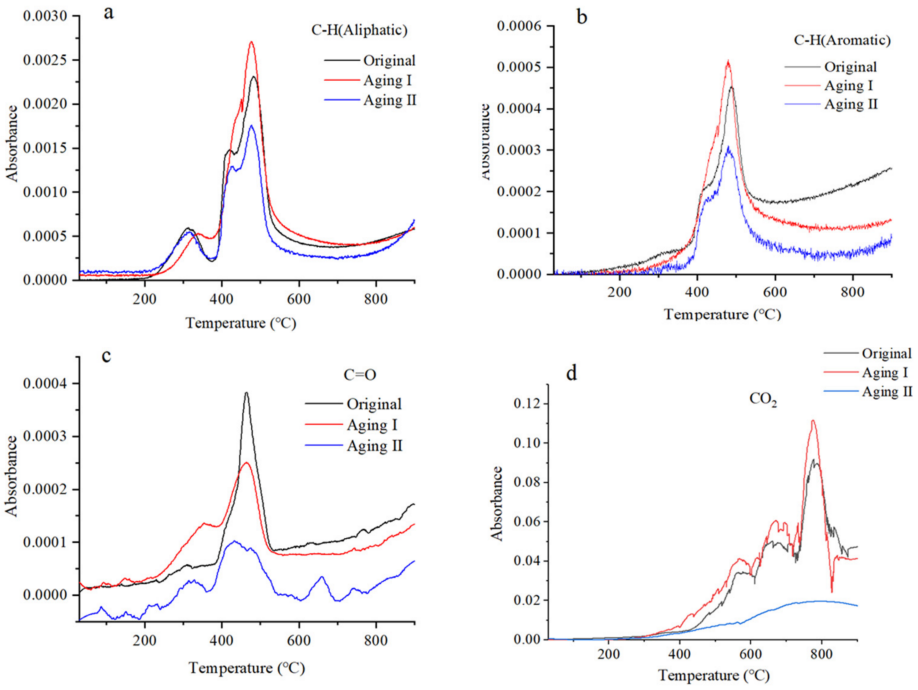

Figure 4. The dynamic changes in FTIR absorbance of C-H (aliphatic) (**a**), C-H (aromatic) (**b**), C=O (carbonyl) compounds (**c**) and CO_2 with pyrolysis temperature (**d**).

The emission process of aliphatic compounds (C-H) (2932 cm^{-1}) from original TWPs can be divided into three stages of 200–400 °C, 400–600 °C, and 600–900 °C, corresponding to polyurethane, rubber and residual isocyanate, respectively [49]. The bond of C-H absorbance peak from TWPs under aging I began at a higher pyrolysis temperature compared to original samples (Figure 4a). This is probably due to the increase in crosslinking density of rubber components caused by thermo-oxidative aging. Compared to original TWPs, the emission amount of aliphatic compounds (C-H) increased under aging I condition, whereas it decreased under aging II condition during the pyrolysis temperature range of 330–900 °C (Figure 4a). This indicated that different components in TWPs have different responses to thermo-oxidative aging. It was speculated that polyurethane in TWPs under aging I condition generated isocyanates with high heat resistance, and their emission amount was higher than that of the original sample at the pyrolysis temperature of 330–900 °C. However, isocyanates in TWPs under aging II may start to be partially decomposed due to the increase of thermo-oxygen aging time, and thus their emission amount was lower than the original samples at 400–600 °C and 600–900 °C.

In addition, in terms of aromatic compounds (C-H bond) (3067 cm^{-1}) in TWPs, their emission amount was the highest at 400–600 °C compared to the pyrolysis temperature of

0–400 °C and 600–900 °C (Figure 4b), which was mainly attributed to the decomposition of synthetic rubber and isocyanate at 400–600 °C [50]. From 500 to 900 °C, the release of aromatic compounds (C-H) gradually decreased with the increase in aging degree of TWPs. Prior studies have reported that the release of aromatic compounds (C-H) at 600 °C was mainly due to the further decomposition of pyrolytic products from rubber [50]. Thus, it can be speculated that the rubber in TWPs after aging was partially degraded, which might cause a decrease in the number of pyrolytic products from rubber, resulting in a relatively lower release of C-H bonds in comparison to the original ones.

The dynamic evolution in pyrolysis release of carbonyl compounds (C=O) (1715 cm^{-1}) also exhibited differences among TWP samples under different aging conditions (Figure 4c). The release amount of carbonyl compounds in aged TWPs was significantly less than in the original ones, and it gradually decreased with aging time (Figure 4c). In general, the carbonyl compounds are mainly sourced from the decomposition of polyurethane and synthetic rubber in TWPs [42]. In this study, under the aging conditions, a large amount of small molecules from polyurethane degradation might have been released, such as esters and carboxylic acid [51], leading to the reduction of carbonyl content in the pyrolysis process.

The initial temperature of CO_2 emission from the aged TWPs (aging I and aging II) was higher than the original TWPs (150 °C), which might be attributed to the additives in aged TWPs being partially decomposed during thermal aging [52]. In terms of emission amounts of CO_2, TWPs under aging I condition possessed the highest amount, followed by original TWPs, and the amount of CO_2 from the sample with aging II was the lowest. The emission of CO_2 in the present study might be mainly due to the decomposition of polyurethane, rubber and isocyanates [52,53]. The oxidation reaction of TWPs under aging I condition might generate a large number of oxygen group elements, leading to the increase of CO_2 emission amount during TG pyrolysis. The thermal oxygen aged TWPs would have higher O contents than the original TWPs. A higher O/C ratio indicates more O-containing functional groups; therefore, pyrolysis products of aged TWPs contained more O-containing compounds [54]. However, with increases in aging time (Aging II), part of CO_2 was generated and released from TWPs, resulting in a decrease in CO_2 amount during TG pyrolysis. In short, different components of tires presented different responses to the thermal aging process, leading to a change in the decomposition temperature and emission amounts of different pyrolytic compound.

3.3. Identification and Dynamics on Gas Components of TWPs with Pyrolysis Temperature

In order to determine the chemical compounds of the synthesized volatile products during the pyrolysis process, GC–MS analysis was used. According to the DTG curve, the released amounts of gas products from TWPs under different aging conditions were the most at around a pyrolysis temperature of 484 °C. Therefore, the gas products released at 484 °C were collected and identified using GC-MS. The chromatograms of the total ionic intensity of the volatile products from TWP pyrolysis at 484 °C are illustrated in Figure S4. The main pyrolysis products of TWPs at 484 °C are shown in Table 1. The results showed that the main products were toluene, m-xylene, styrene, D-limonene, and 7-butyl-2-caprolactone, which were consistent with previous studies [30,55]. The possible major mechanisms of TWP pyrolysis based on these dominant products are shown in Figure 5. In general, rubber was first degraded to produce small olefin and cycloolefin molecules due to chain breaking at lower pyrolysis temperatures [30]. Subsequently, the released olefin and cycloolefin underwent a series of reactions with the pyrolysis temperature rising, including Diels–Alder reactions, cyclization reactions and aromatization reactions, leading to production of benzene and its derivatives [30]. The pyrolysis of polyurethane mainly included the decomposition of polyurethane groups, polyols and isocyanates, as well as 7-butyl-2-caprolactone [51,56].

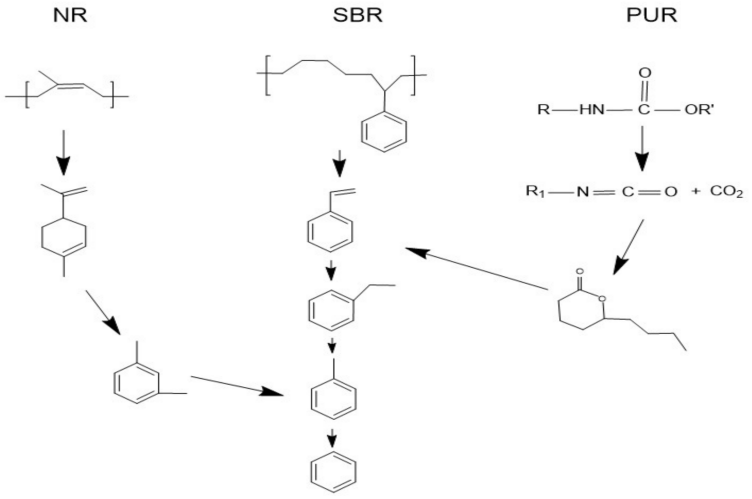

Figure 5. The possible major mechanisms of the TWP pyrolysis (NR, natural rubber; SBR, butadiene styrene rubber; PUR, polyurethane rubber).

Table 1. Specific volatile products identified by MS in helium.

Chemical Formula	Compounds Name	Atomic Mass	Onset/°C			Peak/°C		
			Origin	AgingI	AgingII	Origin	AgingI	AgingII
C_7H_8	Methylbenzene	92	346	335	340	476	470	470
C_8H_{10}	m-Xylene	106	373	373	373	470	464	460
C_8H_8	Styrene	104	381	371	356	476	437	460
$C_{10}H_{16}$	D-Limonene	136	366	366	366	409	409	403

Furthermore, four main gaseous products, including methylbenzene, styrene, m-xylene, and D-limonene were selected for investigation of the dynamic differences in ion currents of gaseous products among different aging stages of TWPs (as shown in Figure 6). Semi-quantitative comparison was conducted after ionic intensity was normalized to equal sample weight before analysis. The amount of styrene released from TWPs under the two aging conditions was higher than that of the original TWPs during TG pyrolysis (Figure 6b). This further demonstrated isocyanate generation due to polyurethane decomposition considering that isocyanates can also be decomposed into styrene [57]. In general, the presence of benzene and its derivatives was caused by the dehydration condensation reaction of isocyanates decomposed from polyurethane polymers. Polyurethane has been reported to be primarily formed by the polymerization of isocyanates and polyols [30]. Furthermore, the amount of styrene released from TWPs under Aging I was higher than that under Aging II, indicating that the isocyanate in TWP would be partly decomposed under Aging II. Similarly, the emission amount of methylbenzene and m-xylene in aged TWP was also much higher than that of the original samples during the TG pyrolysis (Figure 6a,c), which is also attributed to the decomposition of isocyanate during TWP aging [58].

D-limonene was analyzed and we found that the temperature range for D-limonene emission in original and aged TWPs was 366–527 °C (Figure 6d), which coincided with the temperature intervals of fitting peak II (natural rubber) and fitting peak III (synthetic rubber) in the DTG curve (Figure 2c). It can be inferred that D-limonene emission might be due to decomposition of natural rubber and synthetic rubber. Limonene has been considered as a main decomposition product through breaking and intramolecular cyclization processes of natural rubber and styrene butadiene rubber [59]. The structure of D-limonene is generally unstable, and can cause a series of reactions during pyrolysis, easily being converted to other isomers (e.g., 1-methyl-4-(1-methylethylidene) cyclohexene) [30]. With the increase of pyrolysis temperature (>450 °C, Figure 6d), D-limonene forms small molecular substances

(e.g., xylene and benzene due to the cleavage of allyl) [30,49]. Therefore, the content of D-limonene decreased after 400 °C and the increased proportions of xylene and benzene at high temperatures were most likely due to the conversion of limonene in the present study. Furthermore, the emission amount of D-limonene in TWP after Aging I and II was significantly lower than that of the original TWPs during TG pyrolysis, which may be due to the content loss of rubber components in TWPs due to oxidative degradation during the aging process.

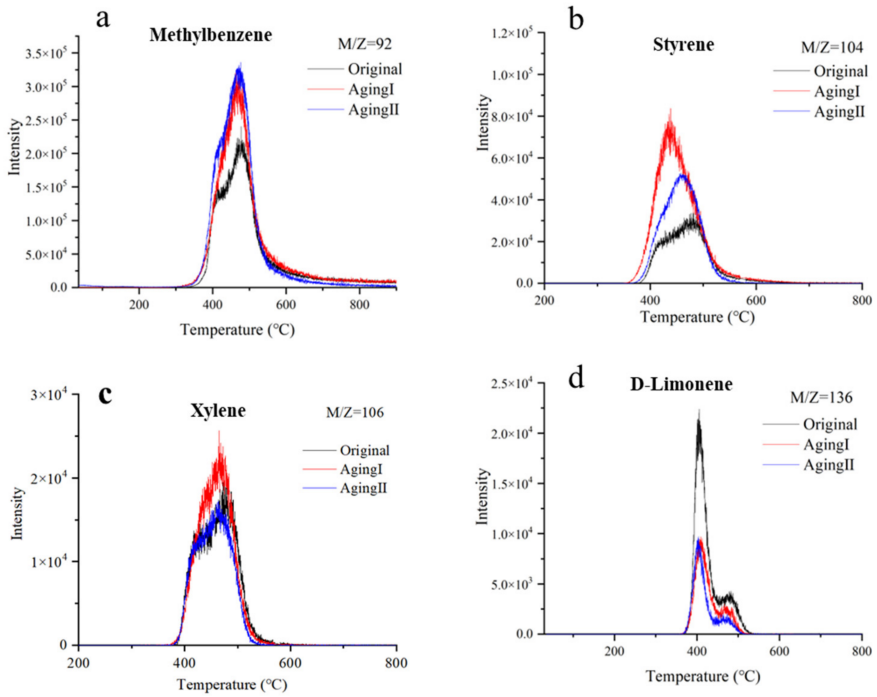

Figure 6. The ion currents of gas products sourced from the pyrolysis process of TWPs with pyrolysis temperatures. ((**a**), the ion currents of methylbenzene; (**b**), the ion currents of styrene; (**c**), the ion currents of m-xylene; (**d**), the ion currents of D-limonene)

According to the above results, it can be speculated that the aged TWPs would release some gas products during the aging process (400 °C). The amount of some gas products (such as D-limonene) from aged TWPs to decreased compared to the original ones at 400 °C during analysis of TG-FTIR-GC/MS (see Figure 6d). This suggested that the aged TWPs would pose potential risks to aquatic and terrestrial ecosystems due to chemical release in the environment. In addition, at higher pyrolysis temperatures of >400 °C by TG-FTIR-GC/MS, some gas products, such as methylbenzene, styrene and xylene, released more amounts from aged TWPs compared to the unaged ones. This suggested that the aged TWPs generated higher amounts of gas products (e.g., styrene, methylbenzene and xylene) in comparison to the original ones in the process of high-temperature pyrolysis, which would lead to potential hazards in the disposal (such as combustion or heat treatment) of waste tires after recycling. In short, TGA-FTIR-GC/MS is a helpful technique for the analysis of real-time pyrolysis dynamics of thermally aged TWPs.

4. Conclusions

The main pyrolysis process in tires involves the decomposition of urethane groups, natural rubbers, synthetic rubbers and isocyanates, as well as further cracking of pyrolysis products. The FTIR analysis indicated that the main pyrolysis gases included CO_2, carbon monoxide, aliphatic compounds, aromatic compounds and carbonyl compounds. The GC/MS analysis further determined the main pyrolytic products, including methylbenzene, styrene, m-xylene and D-limonene. After thermal aging, the dynamics of different types

of products were significantly different. Firstly, the residue rate increased with thermo-oxidative aging. Secondly, short-term thermo-oxidative aging caused an increase in the released amount of aliphatic/aromatic compounds and CO_2 from TWPs, but decreased in terms of long-term thermo-oxidative aging. Moreover, the aged TWPs, especially short-term aged ones, presented higher released amounts of styrene and toluene but lower released amounts of D-limonene compared to the original TWPs. Further research needs to be emphasized on MP release and their environmental fate and potential risk of TWPs during thermo-oxidative aging.

Supplementary Materials: The following supporting information can be downloaded at: https://www.mdpi.com/article/10.3390/w15101944/s1, Figure S1: Morphologies of WTPs with different thermal-oxidative aging time; Figure S2: Changes in ART-FTIR spectra of WTPs with different thermal aging time; Figure S3: 3D FTIR spectra of pyrolysis products of WTPs in original stage (a), aging I (b) and aging II (c); Figure S4: Pyrochromatograph detection of volatile products at 484 °C; Table S1: Characteristic IR absorption bands and functional groups of tires; Text S1: The description on the morphologies of WTPs.

Author Contributions: Conceptualization, X.P. and Q.Z.; methodology, X.P.; software, J.F.; validation, J.F., Q.Z. and X.P.; formal analysis, G.B.; investigation, J.F.; resources, G.B.; data curation, G.B.; writing—original draft preparation, G.B.; writing—review and editing, Q.Z. and X.P.; visualization, G.B.; supervision, X.P.; project administration, X.P. and Q.Z.; funding acquisition, X.P. and Q.Z. All authors have read and agreed to the published version of the manuscript.

Funding: This research was funded by Zhejiang Province Natural Science Foundation (LQ22D010010) and National Natural Science Foundation of China (42207033).

Data Availability Statement: Data are available on demand from the corresponding author.

Acknowledgments: We would like to extend special thanks to the editor and the anonymous reviewers for their valuable comments in significantly improving this paper's quality.

Conflicts of Interest: The authors declare no conflict of interest.

References

1. Andersson-Sköld, Y.; Johannesson, M.; Gustafsson, M.; Järlskog, I.; Lithner, D.; Polukarova, M.; Strömvall, A.-M. *Microplastics from Tyre and Road Wear: A Literature Review*; Swedish National Road and Transport Research Institute (VTI): Linköping, Sweden, 2020; pp. 1–133. [CrossRef]
2. Bostock, J. *Global Industry Tire Volume to Reach 2.7 Bilion Units by 2022*; Smithers: Akron, OH, USA, 2021; pp. 1–2.
3. Wagner, S.; Hüffer, T.; Klöckner, P.; Wehrhahn, M.; Hofmann, T.; Reemtsma, T. Tire wear particles in the aquatic environment—A review on generation, analysis, occurrence, fate and effects. *Water Res.* **2018**, *139*, 83–100. [CrossRef] [PubMed]
4. Youn, J.S.; Kim, Y.M.; Siddiqui, M.Z.; Watanabe, A.; Han, S.; Jeong, S.; Jung, Y.-W.; Jeon, K.-J. Quantification of tire wear particles in road dust from industrial and residential areas in Seoul, Korea. *Sci. Total Environ.* **2021**, *784*, 147177. [CrossRef] [PubMed]
5. Buss, A.H.; Kovaleski, J.L.; Pagani, R.N.; da Silva, V.L.; Silva, J.D.M. Proposal to reuse rubber waste from end-of-life tires using thermosetting resin. *Sustainability* **2019**, *11*, 6997. [CrossRef]
6. Sułkowski, W.W.; Danch, A.; Moczyński, M.; Radoń, A.; Sułkowska, A.; Borek, J. Thermogravimetric study of rubber waste-polyurethane composites. *J. Therm. Anal. Calorim.* **2004**, *78*, 905–921. [CrossRef]
7. Khan, F.R.; Halle, L.L.; Palmqvist, A. Acute and long-term toxicity of micronized car tire wear particles to Hyalella azteca. *Aquat. Toxicol.* **2019**, *213*, 105216. [CrossRef]
8. Järlskog, I.; Strömvall, A.-M.; Magnusson, K.; Gustafsson, M.; Polukarova, M.; Galfi, H.; Aronsson, M.; Andersson-Sköld, Y. Occurrence of tire and bitumen wear microplastics on urban streets and in sweepsand and washwater. *Sci. Total Environ.* **2020**, *729*, 138950. [CrossRef]
9. Unice, K.M.; Kreider, M.L.; Panko, J.M. Comparison of Tire and Road Wear Particle Concentrations in Sediment for Watersheds in France, Japan, and the United States by Quantitative Pyrolysis GC/MS Analysis. *Environ. Sci. Technol.* **2013**, *47*, 8138–8147. [CrossRef]
10. Grigoratos, T.; Martini, G. Brake wear particle emissions: A review. *Environ. Sci. Pollut. Res. Int.* **2015**, *22*, 2491–2504. [CrossRef]
11. Baldwin, J.M.; Bauer, D.R.; Ellwood, K.R. Rubber aging in tires. Part 1, Field results. *Polym. Degrad. Stab.* **2007**, *92*, 103–109. [CrossRef]
12. Carli, L.N.; Bianchi, O.; Mauler, R.S.; Crespo, J.S. Accelerated aging of elastomeric composites with vulcanized ground scraps. *J. Appl. Polym. Sci.* **2012**, *123*, 280–285. [CrossRef]

13. Wagner, S.; Klöckner, P.; Reemtsma, T. Aging of tire and road wear particles in terrestrial and freshwater environments—A review on processes, testing, analysis and impact. *Chemosphere* **2022**, *288*, 132467. [CrossRef] [PubMed]
14. Li, Y.; Zuo, S.; Lei, L.; Yang, X.; Wu, X. Analysis of impact factors of tire wear. *J. Vib. Control* **2011**, *18*, 833–840. [CrossRef]
15. Mathissen, M.; Scheer, V.; Vogt, R.; Benter, T. Investigation on the potential generation of ultrafine particles from the tire–road interface. *Atmos. Environ.* **2011**, *45*, 6172–6179. [CrossRef]
16. Fan, X.; Gan, R.; Liu, J.; Xie, Y.; Xu, D.; Xiang, Y.; Su, J.; Teng, Z.; Hou, J. Adsorption and desorption behaviors of antibiotics by tire wear particles and polyethylene microplastics with or without aging processes. *Sci. Total Environ.* **2021**, *771*, 145451. [CrossRef] [PubMed]
17. Jung, U.; Choi, S.-S. Variation in Abundance Ratio of Isoprene and Dipentene Produced from Wear Particles Composed of Natural Rubber by Pyrolysis Depending on the Particle Size and Thermal Aging. *Polymers* **2023**, *15*, 929. [CrossRef]
18. Kim, D.; Ahn, B.; Ryu, G.; Hwang, K.; Song, S.; Kim, W. Effect of Vinyl Group Content of the Functionalized Liquid Butadiene Rubber as a Processing Aid on the Properties of Silica Filled Rubber Compounds. *Elastomers Compos.* **2021**, *56*, 152–163. [CrossRef]
19. Wang, Z.; Wei, R.; Wang, X.; He, J.; Wang, J. Pyrolysis and combustion of polyvinyl chloride (PVC) sheath for new and aged cables via thermogravimetric analysis-Fourier transform infrared (TG-FTIR) and calorimeter. *Materials* **2018**, *11*, 1997. [CrossRef]
20. Ding, J.; Lv, M.; Zhu, D.; Leifheit, E.F.; Chen, Q.-L.; Wang, Y.-Q.; Chen, L.-X.; Rillig, M.C.; Zhu, Y.-G. Tire wear particles: An emerging threat to soil health. *Crit. Rev. Environ. Sci. Technol.* **2023**, *53*, 239–257. [CrossRef]
21. Liu, Y.; Zhou, H.; Yan, M.; Liu, Y.; Ni, X.; Song, J.; Yi, X. Toxicity of tire wear particles and the leachates to microorganisms in marine sediments. *Environ. Pollut.* **2022**, *309*, 119744. [CrossRef]
22. Veerasingam, S.; Ranjani, M.; Venkatachalapathy, R.; Bagaev, A.; Mukhanov, V.; Litvinyuk, D.; Mugilarasan, M.; Gurumoorthi, K.; Guganathan, L.; Aboobacker, V.M.; et al. Contributions of Fourier transform infrared spectroscopy in microplastic pollution research: A review. *Crit. Rev. Environ. Sci. Technol.* **2021**, *51*, 2681–2743. [CrossRef]
23. Zhang, X.; Zhang, H.; Yu, K.; Li, N.; Liu, Y.; Liu, X.; Zhang, H.; Yang, B.; Wu, W.; Gao, J.; et al. Rapid Monitoring Approach for Microplastics Using Portable Pyrolysis-Mass Spectrometry. *Anal. Chem.* **2020**, *92*, 4656–4662. [CrossRef] [PubMed]
24. Xu, J.; Thomas, K.V.; Luo, Z.; Gowen, A.A. FTIR and Raman imaging for microplastics analysis: State of the art, challenges and prospects. *TrAC Trends Anal. Chem.* **2019**, *119*, 115629. [CrossRef]
25. Kim, J.; Wi, E.; Moon, H.; Son, H.; Hong, J.; Park, E.; Kwon, J.-T.; Seo, D.Y.; Lee, H.; Kim, Y. Quantitative analysis of the concentration of nano-carbon black originating from tire-wear particles in the road dust. *Sci. Total Environ.* **2022**, *842*, 156830. [CrossRef] [PubMed]
26. Thomas, J.; Cutright, T.; Pugh, C.; Soucek, M.D. Quantitative assessment of additive leachates in abiotic weathered tire cryogrinds and its application to tire wear particles in roadside soil samples. *Chemosphere* **2023**, *311*, 137132. [CrossRef]
27. Luo, H.; Zhao, Y.; Li, Y.; Xiang, Y.; He, D.; Pan, X. Aging of microplastics affects their surface properties, thermal decomposition, additives leaching and interactions in simulated fluids. *Sci. Total Environ.* **2020**, *714*, 136862. [CrossRef]
28. Yousef, S.; Eimontas, J.; Striūgas, N.; Mohamed, A.; Abdelnaby, M.A. Morphology, compositions, thermal behavior and kinetics of pyrolysis of lint-microfibers generated from clothes dryer. *J. Anal. Appl. Pyrolysis* **2021**, *155*, 105037. [CrossRef]
29. Nel, H.A.; Chetwynd, A.J.; Kelly, C.A.; Stark, C.; Valsami-Jones, E.; Krause, S.; Lynch, I. An Untargeted Thermogravimetric Analysis-Fourier Transform Infrared-Gas Chromatography-Mass Spectrometry Approach for Plastic Polymer Identification. *Environ. Sci. Technol.* **2021**, *55*, 8721–8729. [CrossRef]
30. Tang, X.; Chen, Z.; Liu, J.; Chen, Z.; Xie, W.; Evrendilek, F.; Buyukada, M. Dynamic pyrolysis behaviors, products, and mechanisms of waste rubber and polyurethane bicycle tires. *J. Hazard. Mater.* **2021**, *402*, 123516. [CrossRef]
31. Chen, J.H.; Chen, K.S.; Tong, L.Y. On the pyrolysis kinetics of scrap automotive tires. *J. Hazard. Mater.* **2001**, *84*, 43–55. [CrossRef]
32. Idris, R.; Chong, C.T.; Asik, J.A.; Ani, F. N. Optimization studies of microwave-induced co-pyrolysis of empty fruit bunches/waste truck tire using response surface methodology. *J. Clean. Prod.* **2020**, *244*, 118649. [CrossRef]
33. Gwaily, S.E.; Badawy, M.M.; Hassan, H.H.; Madani, M. Influence of thermal aging on crosslinking density of boron carbide/natural rubber composites. *Polym. Test.* **2003**, *22*, 3–7. [CrossRef]
34. Liu, J.; Li, X.; Xu, L.; Zhang, P. Investigation of aging behavior and mechanism of nitrile-butadiene rubber (NBR) in the accelerated thermal aging environment. *Polym. Test.* **2016**, *54*, 59–66. [CrossRef]
35. Xu, F.; Wang, B.; Yang, D.; Ming, X.; Jiang, Y.; Hao, J.; Qiao, Y.; Tian, Y. TG-FTIR and Py-GC/MS study on pyrolysis mechanism and products distribution of waste bicycle tire. *Energy Convers. Manag.* **2018**, *175*, 288–297. [CrossRef]
36. Song, P.; Wu, X.; Wang, S. Effect of styrene butadiene rubber on the light pyrolysis of the natural rubber. *Polym. Degrad. Stab.* **2018**, *147*, 168–176. [CrossRef]
37. Jiao, L.; Xiao, H.; Wang, Q.; Sun, J. Thermal degradation characteristics of rigid polyurethane foam and the volatile products analysis with TG-FTIR-MS. *Polym. Degrad. Stab.* **2013**, *98*, 2687–2696. [CrossRef]
38. Chen, R.; Lun, L.; Cong, K.; Li, Q.; Zhang, Y. Insights into pyrolysis and co-pyrolysis of tobacco stalk and scrap tire: Thermochemical behaviors, kinetics, and evolved gas analysis. *Energy* **2019**, *183*, 25–34. [CrossRef]
39. Hu, Q.; Tang, Z.; Yao, D.; Yang, H.; Shao, J.; Chen, H. Thermal behavior, kinetics and gas evolution characteristics for the co-pyrolysis of real-world plastic and tyre wastes. *J. Clean. Prod.* **2020**, *260*, 121102. [CrossRef]
40. Fernández-Berridi, M.J.; González, N.; Mugica, A.; Bernicot, C. Pyrolysis-FTIR and TGA techniques as tools in the characterization of blends of natural rubber and SBR. *Thermochim. Acta* **2006**, *444*, 65–70. [CrossRef]

41. Pagacz, J.; Hebda, E.; Michałowski, S.; Ozimek, J.; Sternik, D.; Pielichowski, K. Polyurethane foams chemically reinforced with POSS—Thermal degradation studies. *Thermochim. Acta* **2016**, *642*, 95–104. [CrossRef]
42. Yang, R.; Wang, B.; Li, M.; Zhang, X.; Li, J. Preparation, characterization and thermal degradation behavior of rigid polyurethane foam using a malic acid based polyols. *Ind. Crops Prod.* **2019**, *136*, 121–128. [CrossRef]
43. Colom, X.; Carrillo, F.; Cañavate, J. Composites reinforced with reused tyres: Surface oxidant treatment to improve the interfacial compatibility. *Compos. A Appl. Sci. Manuf.* **2007**, *38*, 44–50. [CrossRef]
44. Liu, X.; Zhao, J.; Yang, R.; Iervolino, R.; Barbera, S. Effect of lubricating oil on thermal aging of nitrile rubber. *Polym. Degrad. Stab.* **2018**, *151*, 136–143. [CrossRef]
45. Colom, X.; Faliq, A.; Formela, K.; Cañavate, J. FTIR spectroscopic and thermogravimetric characterization of ground tyre rubber devulcanized by microwave treatment. *Polym. Test.* **2016**, *52*, 200–208. [CrossRef]
46. Lei, W.U.; Zhu, S.; University, M.T. Quantitative Study on Tire Aging Based on Characteristic Peak Fitting Method. *China Rubber Ind.* **2017**, *8*, 52–56.
47. Zhang, J.; Wang, C.; Chen, F.; Zao, W.; Feng, H.; Zhao, Y. Thermal-oxidative aging behaviors of shape memory nitrile butadiene rubber composite with dual crosslinking networks. *Polym. Degrad. Stab.* **2020**, *179*, 109280. [CrossRef]
48. De Monléon, Q.; Banet, P.; Chikh, L.; Fichet, O. Effects of pyromellitidiimide pattern on thermomechanical properties and thermal stability of silicone networks. *Polym. Degrad. Stab.* **2022**, *206*, 110187. [CrossRef]
49. Ding, K.; Zhong, Z.; Zhang, B.; Song, Z.; Qian, X. Pyrolysis Characteristics of Waste Tire in an Analytical Pyrolyzer Coupled with Gas Chromatography/Mass Spectrometry. *Energy Fuels* **2015**, *29*, 3181–3187. [CrossRef]
50. Rychlý, J.; Lattuati-Derieux, A.; Lavédrine, B.; Matisová-Rychlá, L.; Malíková, M.; Csomorová, K.; Janigová, I. Assessing the progress of degradation in polyurethanes by chemiluminescence and thermal analysis. II. Flexible polyether- and polyester-type polyurethane foams. *Polym. Degrad. Stab.* **2011**, *96*, 462–469. [CrossRef]
51. Eschenbacher, A.; Varghese, R.J.; Weng, J.; Van Geem, K.M. Fast pyrolysis of polyurethanes and polyisocyanurate with and without flame retardant: Compounds of interest for chemical recycling. *J. Anal. Appl. Pyrolysis* **2021**, *160*, 105374. [CrossRef]
52. Chen, X.; Huo, L.; Jiao, C.; Li, S. TG–FTIR characterization of volatile compounds from flame retardant polyurethane foams materials. *J. Anal. Appl. Pyrolysis* **2013**, *100*, 186–191. [CrossRef]
53. He, J.; Jiang, L.; Sun, J.; Lo, S. Thermal degradation study of pure rigid polyurethane in oxidative and non-oxidative atmospheres. *J. Anal. Appl. Pyrolysis* **2016**, *120*, 269–283. [CrossRef]
54. Tian, L.; Shen, B.; Xu, H.; Li, F.; Wang, Y.; Singh, S. Thermal behavior of waste tea pyrolysis by TG-FTIR analysis. *Energy* **2016**, *103*, 533–542. [CrossRef]
55. Kwon, E.; Castaldi, M.J. Fundamental understanding of the thermal degradation mechanisms of waste tires and their air pollutant generation in a N2 atmosphere. *Environ. Sci. Technol.* **2009**, *43*, 5996–6002. [CrossRef] [PubMed]
56. Khaleel, M.; Soykan, U.; Çetin, S. Influences of turkey feather fiber loading on significant characteristics of rigid polyurethane foam: Thermal degradation, heat insulation, acoustic performance, air permeability and cellular structure. *Constr. Build. Mater.* **2021**, *308*, 125014. [CrossRef]
57. He, Y.; Chen, X.; Tang, X.; Chen, S.; Evrendilek, F.; Chen, T.; Dai, W.; Liu, J. Co-combustion dynamics and products of textile dyeing sludge with waste rubber versus polyurethane tires of shared bikes. *J. Environ. Chem. Eng.* **2023**, *11*, 109196. [CrossRef]
58. Šourková, M.; Adamcová, D.; Vaverková, M.D. The influence of microplastics from ground tyres on the acute, subchronical toxicity and microbial respiration of soil. *Environments* **2021**, *8*, 128. [CrossRef]
59. Arockiasamy, A.; Toghiani, H.; Oglesby, D.; Horstemeyer, M.F.; Bouvard, J.-L.; King, R.L. TG–DSC–FTIR–MS study of gaseous compounds evolved during thermal decomposition of styrene-butadiene rubber. *J. Therm. Anal. Calorim.* **2013**, *111*, 535–542. [CrossRef]